Progress In Electromagnetics Research, PIER 69, 177–200, 2007

EIGENWAVE CHARACTERISTICS OF A PERIODIC IRIS-LOADED CIRCULAR WAVEGUIDE. THE CONCEPTS

S. K. Katenev

Theoretical Radiophysics Department
V. N. Karazin Kharkov National University
Kharkov, Ukraine

Abstract—The eigenwave dispersion (its initial periodicity-dispersion component) and the H_{0i}-wave power flows (via the partial wave concept proven) are examined in a periodic iris-loaded circular waveguide (PICW). The eigen-values and modes are classified; arbitrariness of a Bragg wave-point location, the eigenwave interpretation, the contra-directional power flows, the asymmetric wave hybridity, and etc., are found and/or explained. All of the results are valid to the class of periodic-boundary structures (PBS).

1. NOTATIONS LIST PERTAINING TO THE PROBLEM

1. $(\kappa_B, \kappa\alpha_B) \equiv (\kappa, \kappa\alpha)_B$ — Bragg wave-number and its ordinate on the Brillouin plane $(\kappa, \kappa\alpha)$, i.e., the Bragg wave-point;
2. $\Delta\omega_B$ — Bragg band, i.e., a (locally) forbidden band; $\Delta\Omega_i$ — the i-mode propagation band;
3. *periodicity dispersion* — the first one of the two factors — periodicity and diffraction — responsible for the waveguide dispersion forming;
4. *initial periodicity dispersion (i.p.d.)* — the waveguide dispersion at infinitesimal irises;
5. *regular mode* — the PICW eigenmode in one-to-one correspondence to that of the smooth waveguide;
6. *periodicity mode* — the PICW eigenmode originating due to the periodicity effect;
7. *partial waves* — the independent ingredients of a PICW eigenwave.

2. INTRODUCTION

There is hardly any need to say much about the importance of periodic structures in connection to electromagnetic wave theory and applications. Here the analysis of the axially-symmetric periodic waveguides and structures is an important branch. Among them a periodic iris-loaded circular waveguide, Fig. 1, can be treated, to some extent, as a canonical example and a focal point of analysis. This is due to its traditionally important and numerous applications in the linear accelerators of electrons [1–12], microwave tubes [13–16], and antenna technology [17–19].

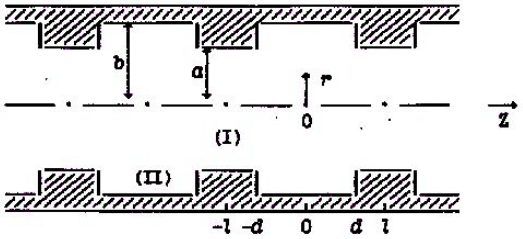

Figure 1. Periodic iris-loaded circular waveguide.

The canonic character of PICW is strengthened even more by its simplest geometric shape. We can use it as a starting point to build a theory of more complex-shape structures from the vast class of periodic-boundary structures, both closed and open [20].

Even in view of the most recent more or less generalized advancements as to periodicity, e.g., such as those in [21–25], the adequately treated below eigenwave mode of PICW, or, at least, its certain further developments, could have value.

The research on PICW started as early as the mid-1940's [1–4]. In the next decades, the most intensive studies and applications were in the particle acceleration [5–12, 26]. Other PICW applications were developed later as regards the microwave tubes and other fields.

Nevertheless, electromagnetic theory of PICW is far from completion; mainly because of the extreme complexity of the PICW eigenwaves behavior and the inevitable heavy rigorous computations in this respect.

Such opinion is supported, e.g., by several principal questions left unanswered as yet. 1) Two factors are known to be responsible for the PICW dispersion forming — diffraction and periodicity; but how do they work actually? 2) Which is the total number of eigenmodes in such a waveguide? 3) Which is the exact influence of each single geometric parameter of the waveguide b, l, d, a (Fig. 1) regarding the

eigenmode behavior. 4) What are, in effect, the major characteristic features, qualitative and quantitative, of the PICW eigenwaves.

Besides, certain commonly admitted deficiencies in the PICW eigenwave studies do call for a more in-depth analysis. Namely, 1) it is commonly accepted that in the case of a positive dispersion, the power flow of a positive number space harmonics is in the direction of the eigenwave itself; while for a negative number harmonics, it is in the opposite direction; when the dispersion is negative, it is v.v. [12]. However, this turns out to be not a general rule; while the sets of the negative and the non-negative harmonics do produce the two partial waves, accordingly. 2) Also, there is still an amount of uncertainty about PICW asymmetric eigenwaves. This concerns: a) their definition, e.g., exactly how to call their 1st mode, out of the vast list of options used now — $\{E_{11}, E_{11}/H_{11}, HEM_{11}$ or EH_{11} and etc$\}$. [10, 12]; b) their characteristics of the hybridity; c) the contra-directive to each other length-wise layers of power flows in the eigenwave; d) their mode inversion property; and some others. 3) A good deal of knowledge is still missing on the E_{0i}-waves. E.g., as regards: a) the frequency drift and stability of the modes versus radius a; which is definitively analogous to the asymmetric wave case; b) the mode inversion property; and etc. 4) There is quite a serious lack of knowledge on the H_{0i}-waves, e.g., on their mode inversion characteristic, Bragg bandwidth extremums, and many others [27–28].

And although the general views and approaches as for the periodic structures are known for a long time [29], the partial-wave concept in effect, for example, and all its implications, inlcuding the actual power investigation, are completely unavailable. Besides, a certain update of the available material may have reason.

Not all of these merely asserted points can be properly illustrated in any single paper.

In this paper, the waveguide dispersion and the power flows are considered. There are two basic results, in validity to all of the wave types: 1) on the origination of the dispersion;

2) the partial waves in effect actual investigation.

Beforehand, some relationship of equivalence is to be mentioned. It is a one-to-one reciprocal correspondence, in a wave process with dispersion [30], between the solutions of the wave equation (i.e., its whole set of possible eigenwaves versus the problem's parameters) and the ones of the dispersion equation (i.e., the whole set of its dispersion curves versus the same). Validity of this relationship to PICW provide, e.g., a convenient method at hand for verifying the numerical data due to *the duplicate/no duplicate* alternative between the both types of information. The duplicate does mean verity.

3. ON THE METHOD, SOME ACTUAL TECHNIQUES, AND THE COUPLED WAVE APPROACH

The both factors responsible for the forming of the dispersion in PICW, diffraction and periodicity, are inseparable and not easy to evaluate, and the diffraction acts quite implicitly in the eigenwave mode. The two ways for dealing definitely with this problem are: a certain modeling scheme [31] and Modal Basis Method (MBM) [32, 33]. In order to know about what actually occurs concerning the waves, the straight computations by the conventional coupled regions method [10, 12] (see Fig. 1, where (I) is propagation and (II) periodicity region) succeed fairly well throughout this investigation. The system of harmonic functions $\{\exp(i\pi n/l)z\}, n = 0, \pm1, \pm2, \ldots$, is applied as the basis for Fourier expansions within Region (I). So is the system of functions $\{\cos\psi_m(z),\ \sin\psi_m(z)\}$, where $\psi_m = (\pi m/2d)(z+d-2Nl)\, m = 0, 1, 2, \ldots,\ N = 0, \pm1, \pm2, \ldots$, within Region (II). These computations yield the Brillouin diagrams $\{\kappa = \kappa(\kappa\alpha)\}$, where $\kappa = kl/\pi$; $\kappa\alpha = \kappa\alpha l/\pi$; k is wave number in free space, α is a deceleration coefficient, l is the half-period} and averaged in time Poynting vector $\vec{S}(r, z)$ and power flow P in the waveguide. A number of the facts regarding the PICW wave behavior start getting presented in Section 4.

In order to understand physically the found facts, both the modeling and MBM do prove to be necessary. The modeling scheme adopted is that using the periodic layered circular waveguide, with its purely periodicity dispersion and analytical solution [31]. The diffraction factor can be evaluated using MBM, with its explicit form of the inter-modal diffraction, or of the coupling (see just below), coefficients. Using these both schemes is a work that is under way presently.

The coupled wave approach, or the method of Pierce and Tien waves [34, 35], is a fairly convenient formalism for investigating the waves in periodic structures. In particular, the coupled wave approach works best when the periodicity dispersion [36] is involved [36–38]. But this approach actually inherently fails in PBS, because of the strong diffraction upon the boundaries. But the mere idea of the coupled wave approach is valid under the PICW conditions; the formulation is presented at the end of Section 4.

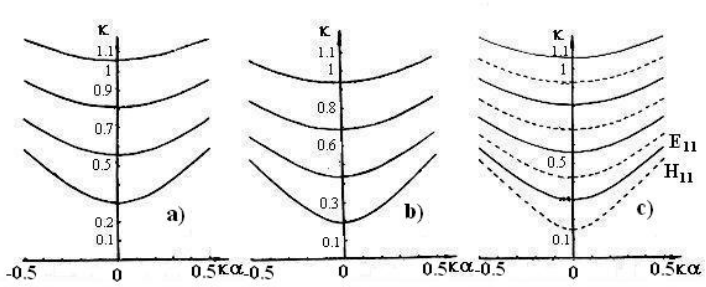

Figure 2. Dispersion curves of the symmetric H_{0i} (a), E_{0i} (b) and the asymmetric H_{1i}, E_{1i} (c) waves of the smooth circular waveguide $b = 3$ (scaled by $l = 0.75$).

4. THE EIGENWAVE MODE AND THE INITIAL PERIODICITY DISPERSION

In Fig. 2 there are the dispersion curves of the smooth circular waveguide: symmetric H_{0i}, a); E_{0i}, b), and asymmetric H_{1i}, E_{1i}, c), $i = 1, 2, 3, 4$ waves. The alteration of H_{1i} and E_{1i} modes in frequency, as is demonstrated below, causally relates to the PICW asymmetric waves hybridity.

At infinitesimal perturbations in the smooth circular waveguide, Fig. 3, diffraction is missing, and the *periodicity* dispersion works alone, in its *initial* mode.

Of PICW parameters $\{l, b, d, a\}$, radiuses b and a are of a certain physical equivalence; b, for instance, can be held constant, e.g., $b \equiv 3$, and only (l, d, a) varied. Also, the generally predominant influence is that by the period l value. In order to most easily evaluate the value $l \in [0, \infty)$ effect, its continuum is to be physically 'poled off' into long and short period values. And of those portions, two typical constant samples have been selected and explored in detail and got compared in between; thus providing quite a satisfactory model on the whole.

The period is to be regarded as the long one when

$$l > \pi b / j'_{02},$$

where j'_{02} is the 2-nd root of Bessel function J_0 derivative, i.e., of function J'_0, when the H_{0i}-waves are concerned; j_{02} substitutes for j'_{02} as for the E_{0i}-waves, and etc.

Thus, the factual limitation of the two sample periods, $l = 3$, $l = 0.75$, at $b \equiv 3$, and the parameters $\{d, a\}$ optimally varied, is applied to represent the general situation in PICW.

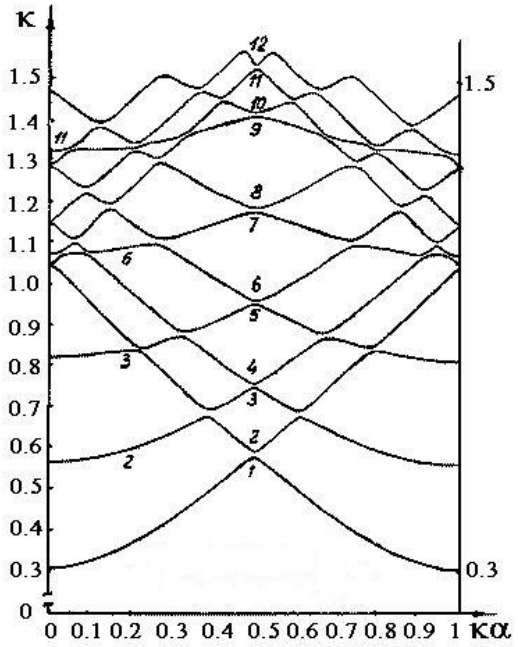

Figure 3. Infinitesimal perturbations in the regular waveguide.

As an example, in Fig. 4, for comparison in the same scale of $0.75/\pi$ and at $a = 2.8$, there are the first 8 eigenmodes H_{0i}, $i = 1, 2, \ldots, 8$, at $l = 3$ and $l = 0.75$ periods, and wide slots between the irises. It is seen from Fig. 4 that any growth of l, the parameter responsible for the Brillouin diagram zone structure, does lead to the growth of the total number of modes in the waveguide. Parameters $\{d, a\}$ are responsible for the less general characteristics, e.g., the Bragg bandwidth extremums, the frequency drift or stability of the modes, and etc.

The term 'zone structure' traces back to the condition by Bragg concerning X-rays diffraction in crystals [20]. In periodic structure theory, analogous relationship, under the same name of Bragg condition, corresponding to number m order, is normally written as

$$\kappa\alpha_B = m/2, \tag{1}$$

where $m = 1, 2, \ldots$ and $\kappa\alpha_B$ are called Bragg wave-numbers [20].

Here, this calling is preserved; the points $(\kappa_B, \kappa\alpha_B) \equiv (\kappa, \kappa\alpha)_B$ are called Bragg wave-points; and their forbidden bands are called Bragg bands, denoted with $\Delta\omega$. The i-mode propagation band is denoted with $\Delta\Omega_i$.

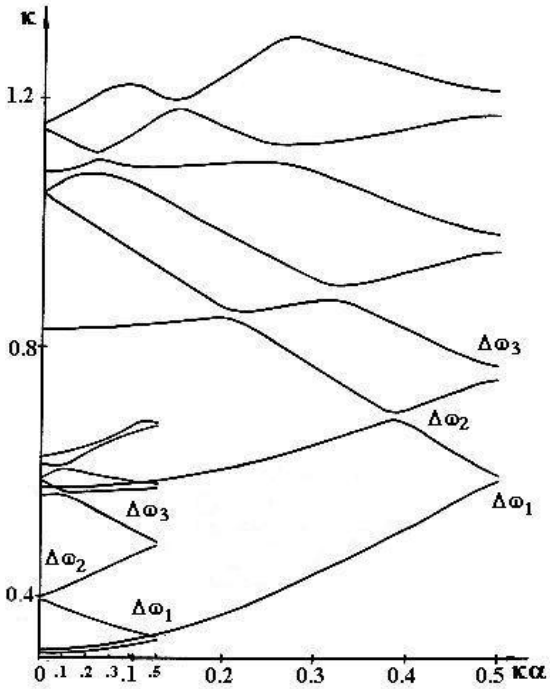

Figure 4. H_{0i}-waves in the waveguides with wide slots $b = 3$, $l \in \{3,\ 0.75\}$, $a = 2.8$; the scale is that by $l = 0.75$.

As functions of $\theta = d/l$, the Bragg bandwidths $\Delta\omega_B(\theta)$ possess extremums, discussed in more detail in [27, 28]. An example is presented in Fig. 5(a) for H_{oi}, $i = 1, 2, 3, 4$; all of the Bragg bands are forbidden bands: $\Delta\omega_i(\theta)$, $i = 1, 3$ at $\kappa\alpha = 0.5$, and $i = 2$ at $\kappa\alpha = 0$ (see Fig. 4, $l = 3$). One more example, using another way of the graphic representation, is shown in Fig. 5(b). There are the lower $\kappa_i'(\theta; a)$ and upper $\kappa_i^u(\theta; a)$ boundaries of $\Delta\omega_i = \kappa_i^u - \kappa_i^l$ at $a \in \{2.8$ -solid, 2.4 -dotted, 2 -dashed lines$\}$. Each a-parameter lowest curve is the cut-off frequency κ_{1c} of H_{01}. Denoting $\kappa_{1c} \equiv \kappa_0^u$, then $\Delta\Omega_i = \kappa_i^l - \kappa_{i-1}^u$. There are i maximums and $i - 1$ minimums in each of the stop bands $\Delta\omega_i(\theta; a)$.

It is commonly admitted [12, 20] that as the eigenwave number approaches a Bragg wave-number, the distributed feedback upon the periodic perturbations (Bragg back-scattering [20]) turns cumulative and the Bragg band is assumed to get formed via summing-up in phase of the successive reflections upon perturbations [12, 20].

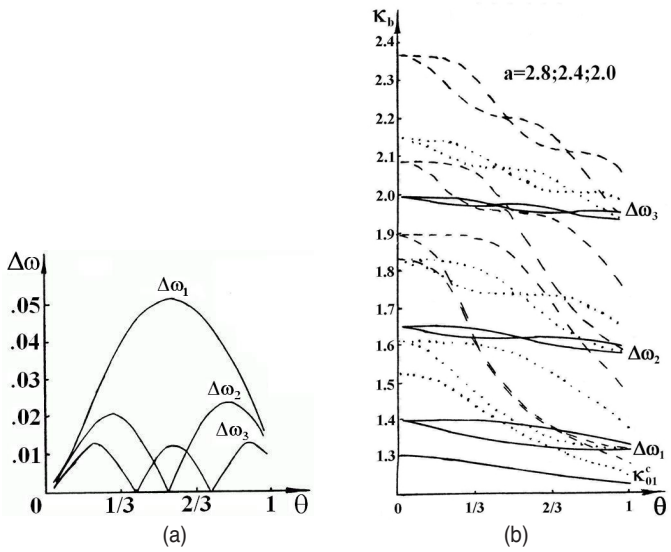

Figure 5. (a) The H_{oi} Bragg bandwidths extremums $\Delta\omega_i(\theta)$, $i = 1, 2, 3$, in the waveguide $l = 3$, $d = 2.8$, $a = 2.8$. (b) The Bragg bandwidths extremums via the boundary frequency representations.

In a periodic-boundary waveguide, there are other than (1) Bragg wave-points; and their number and coordinates are functions primarily of l (see Fig. 4) and of d, a also. Here the following notation is employed: $\kappa\alpha_i^j, \kappa_i^j, \Delta\omega_i^j$. With i is denoted the order number of the (lower) mode; with j, that counts from $\kappa\alpha = 0$, the order number of the mode's Bragg attribute if the mode has more than one such individual attribute.

Thus for the symmetric H_{0i}-waves, the Bragg wave-point $(\kappa\alpha, \kappa)_2^1$ coordinates in the cross-point of the 2-nd branch of 0-tree and the 1-st one of (-1)-tree, Fig. 6, is the solution of the system

$$\begin{cases} \kappa^2 - \kappa\alpha^2 = \tilde{j}'^2_{02}/b^2; \\ \kappa^2 - (1 - \kappa\alpha^2)^2 = \tilde{j}'^2_{02}/b^2; \end{cases} \tag{2}$$

i.e.,

$$\begin{aligned} \kappa\alpha_2^1 &= \left(b^2 + \tilde{j}'^2_{01} - \tilde{j}'^2_{02}\right)/2b^2; \\ \kappa_2^1 &= \left[\left(b^2 + \tilde{j}'^2_{01} + \tilde{j}'^2_{02}\right) - 4\tilde{j}'^2_{01}\tilde{j}'^2_{02}\right]/2b^2, \end{aligned} \tag{3}$$

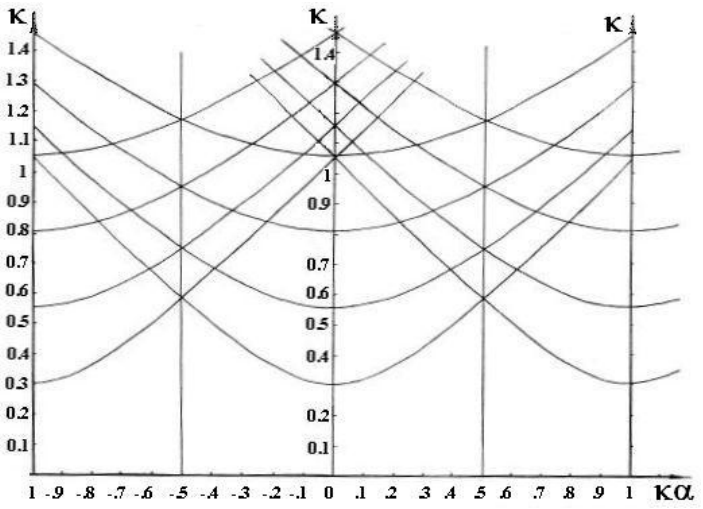

Figure 6. Origination of the initial periodicity dispersion: the fragment of the regular trees set at $\kappa\alpha = 0, \pm 1$.

where $\tilde{j}'_{0m} = j_{om}l/\pi$ is the m-th root, $m = 1, 2, \ldots$, of the Bessel function derivative J'_0.

For other points, e.g., $(\kappa\alpha, \kappa)^1_3$, $(\kappa\alpha, \kappa)^2_3$ in Fig. 3, formula (3) does get generalized by the immediate indices substitution; for, e.g., $(\kappa\alpha, \kappa)^1_4 = (0, \kappa)_4$, the solution is obtainable straightway from (2) as

$$\kappa^1_4 = \left(1 + \tilde{j}'^2_{01}/b^2\right)^{1/2}. \tag{4}$$

For those reasons, and in view of the infinity of κ axis and the arbitrariness of the structure period value (see Fig. 4), the in-phase reflections summing-up idea gets excluded, as a cause for the Bragg wave-point origination in PICW. Indeed, any point $\kappa\alpha \in [0, 0.5]$ can either be strictly a Bragg wave-number itself or lie in some forbidden near-vicinity of such a one; and thus, all the propagation points can be excluded at all. Which holds true here is that any point $\kappa\alpha \in (0, 0.5)$ may be, simultaneously, a Bragg wave-number relating some particular eigenmode as well as a wave number for all the other (infinite number) eigenmodes, except maybe some few. And in this way, the Bragg wave-point origination is to be independent on the wavelength mechanism.

This statement, formulated so far using Brillouin diagrams, farther on duplicates under the energy aspect.

All the points on the eigenmode dispersion curve can divide into three groups: 1) the propagation points of a pass band; 2) the Bragg

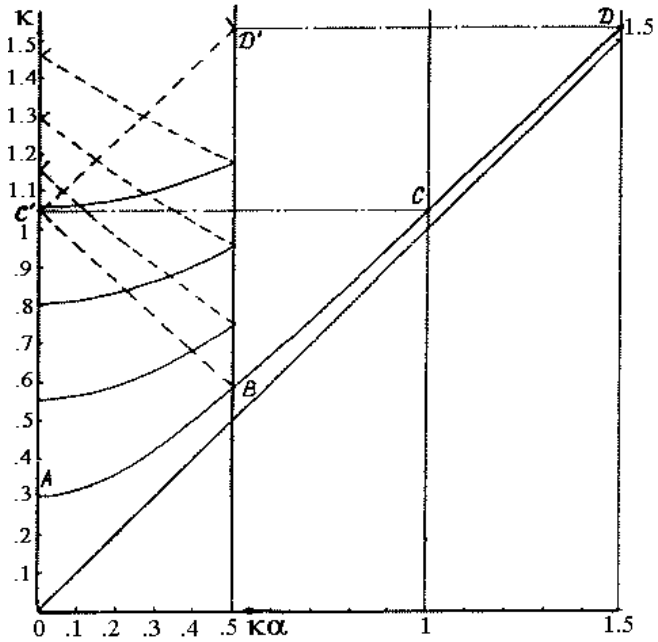

Figure 7. Origination of the initial periodicity dispersion: the isometric representation of the regular dispersion tree from the triangle $\kappa > \kappa\alpha$ into the domain strip $0 \leq \kappa\alpha \leq 0.5$.

wave-points (their set ϕ, as $\kappa\alpha = 0.5$ is such a one); 3) the left ends of the modes, which at infinitesimal perturbations can be either of the type in close vicinity to the regular cut-off frequencies or the type when they are Bragg wave-points.

This modal property 3) is used in order to classify the modes. Let the 1-st type eigenmodes be those in the one-to-one reciprocal correspondence with the regular waveguide modes. The 2-nd type ones are all the rest ones. They have Bragg wave-points at $\kappa\alpha = 0$, and originate in pairs due to the periodicity effect. It is logical to call the 1-st type modes *regular* and the 2-nd type modes *periodicity* ones.

If Fig. 6 and Fig. 7 are compared, the equivalence is seen between two possible patterns of the i.p.d. formation. In the 1-st pattern, the i.p.d. is due to the crossings of the branches of the 'regular' dispersion curve trees $\kappa\alpha = 0, \pm 1$, Fig. 6. In the 2-nd pattern, — as a result of the branches 'bending' and the appropriate displacement of the whole right-hand portion $0 \leq \kappa\alpha < \infty$ of the 'regular" tree $\kappa\alpha = 0$ crown into the domain strip $\{\kappa\alpha \in [0, 0.5], \kappa \in [0, \infty]\}$, Fig. 7.

In this way, the following final statement can get formulated (*on*

the i.p.d. formation).

Infinitesimal perturbations in the regular waveguide result in the isometric representation of the whole set of its dispersion curves out of the triangle $\{\kappa\alpha > 0, \kappa > 0;\ \kappa > \kappa\alpha\}$ **of the Brillouin plain into the strip** $\{\kappa\alpha \in [0, 0.5],\ \kappa \in [0, \infty]\}$**.**

The eigenmode cut-off frequencies are

$$\{k_{cmn}\} = \left\{ \sqrt{\left(\frac{\pi n}{l}\right)^2 + \frac{j'^2_{0m}}{b^2}},\quad n = 0, 1, 2, \ldots, m = 1, 2, \ldots \right\};$$

the regular cut-offs are those at $n = 0$ **and the periodic ones are all the rest.**

The Bragg wave-point frequencies at $\kappa\alpha = 0.5$ **are**

$$\{k_{mn}\} = \left\{ \sqrt{\left(\frac{\pi(n - 0.5)}{l}\right)^2 + \frac{j'^2_{0m}}{b^2}},\quad n = 1, 2, \ldots, m = 1, 2, \ldots \right\}.$$

And the domain strip width is $W = 1/4l$**.**

All of the originated Bragg wave-point coordinates are obtainable either generally numerically using the previous relationships or in analogy to (2)–(4).

The total number of the waveguide eigenmodes is obtainable as

$$N_{TOT} = N_{TOT,R} + N_{TOT,P}(l) = N_{TOT,R} + N^1_{TOT,P} \cdot l, \qquad (5)$$

where $N^1_{TOT,P} = N_{TOT,P}(1)$.

This representation holds all the eigenfrequencies constant everywhere, except in the Bragg wave-points, where they become forbidden at least locally. The piece-wise composed eigenmodes are formed in the Bragg wave-points inside the interval $\kappa\alpha \in (0, 0.5)$; in the asymmetric-wave case this results in these waves' hybridity (see below).

The proof of (5) is found from analyzing Fig. 8 diagram, with its upper plotting. Here are the sequences of the numerically obtained PICW cut-off frequencies for the H_{0i}-waves for six l values within a constant, and sufficiently long bandwidth; which embraces 7 junior regular modes H_{0i}, $i = 1, 2, \ldots, 7$. As the regular modes number i tends to ∞, the angle α in the Fig. 8 plotting will tend to $\pi/2$; and $N = N_R + N_P$ to $N_{TOT} = N_{TOT,R} + N_{TOT,P}$.

N_{TOT} number is independent on d or a parameters.

Relationship (5) is valid to every wave type in a periodic-boundary waveguide.

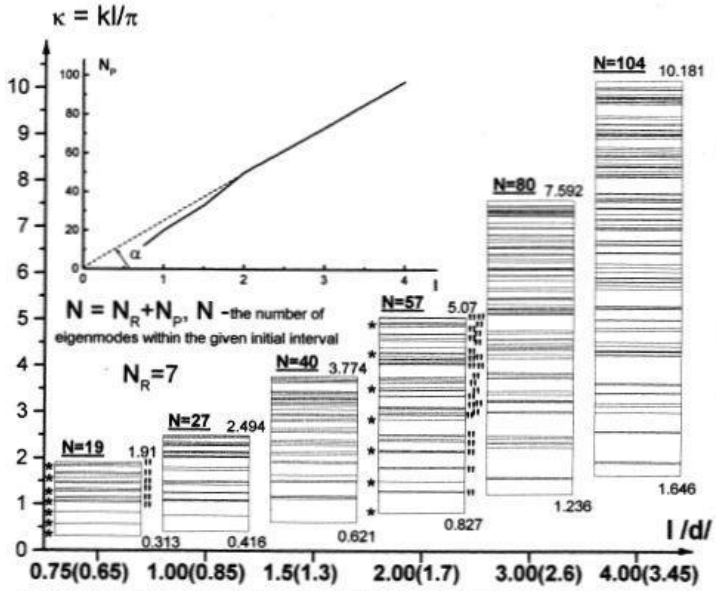

Figure 8. The cut-off frequencies of junior H_{0i}-waves in PICW at 6 period values $l = \{0.75, 1, 1.5, 2, 3, 4\}$ (the corresponding d-values are in parenthesis, $a = 2,\ b = 3$) within the bandwidth $0 < k < 8$ around the first 7 regular modes, denoted with '*'. With '///' are denoted the periodicity modes.

This statement's Brillouin diagram language is just on the transition from the regular to periodic waveguide. The dispersion's periodicity component is responsible alone for the origination of the waves, while the diffraction factor is yet unavailable.

When the irises are arbitrary, we can't separate clearly the periodicity effect from that one by diffraction; the latter, if any, being implicit and, perhaps, negligible. And most probably the partial waves complexity below is, in effect, the produce by the periodicity factor entirely.

Getting back to the coupled wave approach model, the situation in PICW can, in a sense, be regarded as a generalized limit case of this model at: 1) the increase from finiteness to infinity in {a number of the 'coupling elements'} ≡ {the number of 'periodic boundary perturbations'} along the waveguide wall; 2) the propagation within the same room, facing each other, of the two waves interacting/coupled via a multi-scattering from the periodic irises.

This generalization can be a sufficient ground in the *separation* of the negative space harmonics set from the non-negative one in the

power flow analysis below.

5. THE PARTIAL WAVE CONCEPT

The following material is in energy terms; the generalization above is to be a lead. The H_{0i}-waves are involved; comparatively the simplest ones, they are quite revealing in general.

Farther on, the negative, $n < 0$, and non-negative, $n \geq 0$, space harmonic sub-sets are dealt with individually. In so doing, averaged in time eigenwave power flow $P|_{z=\pm 1}$ or Poynting vector $\vec{S}(\vec{r}, z)$ avail of the four portions each like this

$$Q = Q^{-} + Q^{-+} + Q^{+} + Q^{+-}, \quad \left(Q \in P, \vec{S}\right), \tag{6}$$

where the signs '$-$' and '$+$' correspond to the sums $\sum\limits_{n=\infty}^{-1}$, $\sum\limits_{n=0}^{\infty}$ in the individual 'eigen-powers'; and their 'cross-powers' are denoted with double signs, where the 1-st sign pertains to the electric field.

As a pattern to be kept to on, in Fig. 9 are presented, for a weakly perturbed regular waveguide, $l = 3$, $d = 2.285$, $a = 2.4$, H_{01}, $\kappa\alpha = 0.32$, all the four component flows (6) (all referred to further as 'powers') of vector $\vec{S}$, vector $\vec{S}$ itself and vector $\vec{S}_I$ (see on it below). The lowest left-hand corner power flow is the total waveguide power $\vec{S} = \vec{S}_T$, it propagates in the positive direction. The next one above is the reflected power $\vec{S}_R = \vec{S}^{-}$, and the 2nd above is $\vec{S}^{+}$. The right-hand column contains the cross-powers $\vec{S}^{-+}$ and $\vec{S}^{+-}$, and the sum $\vec{S}_I = \vec{S}^{+} + \vec{S}^{-+} + \vec{S}^{+-}$ (T, R, I stand for *transmitted, reflected, initial*). Thus, the following identity gets valid

$$\vec{S}_T(\vec{r}, z) = \vec{S}_I(\vec{r}, z) + \vec{S}_R(\vec{r}, z). \tag{7}$$

When the dispersion is negative $d\kappa/d\kappa\alpha < 0$, the components in (7) are $\vec{S}_I = \vec{S}^{-} + \vec{S}^{-+} + \vec{S}^{+-}$, $\vec{S}_R = \vec{S}^{+}$ where $S_{TZ} < 0$, $S_{IZ} < 0$, $S_{RZ} > 0$.

Analogous relationship is relevant for the waveguide power flow P

$$\left(P_T = P_I + P_R\right)\Big|_{Z=\pm l} \tag{8}$$

This can get generalized for the whole mode as $P^M \approx \int\limits_0^{0.5} P(\kappa\alpha) d\kappa\alpha$.

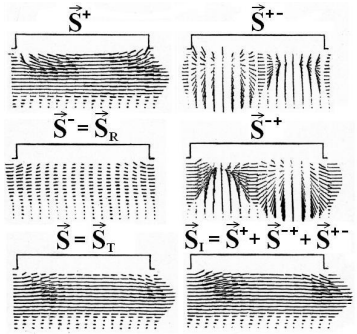

Figure 9. A canonical pattern of the power flow ingredients (6) $\vec{S}$, $\vec{S}^{-}$, $\vec{S}^{+}$, $\vec{S}^{+-}$, $\vec{S}_I = \vec{S} + \vec{S}^{-+} + \vec{S}^{+-}$ in a slightly perturbed waveguide, with a large period, wide slot and thin iris.

First the long period, $l = 3$, and then the short one, $l = 0.75$, are examined. It is not a place to characterize the period-length effect in detail, but would rather briefly like this. Although, in a sense, the long periods are physically simpler, e.g., as they contain the transition to the smooth waveguide on one end (at $l \to \infty$), they generally embody the successive stages of forming all of the wave characteristics, as l decreases. Just because of these 'unstable' processes of the gradual forming, the long periods yield to the numerical calculations of power flows at least one order more difficult compared with the short ones. Physically, the short periods do represent the completely formed-up wave characteristics; namely, for their most part towards $l \to 0$ end. For this reason, they yield to numerical calculations that much better, nearly increasingly better as l decreases.

6. THE LONG PERIODS IN PICW

The power flows (6) in Fig. 9 represent quite a trivial case. Here, the powers $\vec{S}$, $\vec{S}_R = \vec{S}^{-}$ and $\vec{S}_I$ have no curls, i.e., are laminar, $\vec{S}^{+}$ has a small curl around $r = a$. The powers $\vec{S}^{-+}$ and $\vec{S}^{+-}$ have rather complex configurations, and both their flows $P^{+-} < 0$, $P^{-+} > 0$ are r-homogeneous at $z = \pm l$. As d, a parameters of the guide vary, powers (6) turn more complex.

Within the waveguide $d = 2.425$, $a = 2$, mode H_{02}, $(d\kappa/d\kappa\alpha < 0)$, $\kappa\alpha = 0.4$, Fig. 10, the backward powers ($z \to -\infty$) are practically missing, i.e., $P_T P_R > 0$, where $P_R = P^{+}$. Thus, the relationship (7) gets generalized as $P_T = P_R + P_I$. Here, the laminar waveguide total

power is in the role of the initial, and all the rest ones are more complex. All of the powers are co-directional, with a small exception in $\vec{S}^{-}$ near $r = a$. The next simplest is $\vec{S}_I$, with a rotating co-direction to $\vec{S}_I$ curl around $r = a$; the curl around $r = a$ in $\vec{S}_R = \vec{S}^{+}$ is contra-direction in relation to $P_R(z)$. Note quite a weak backward power flow ($z \to -\infty$) in $\vec{S}^{-}$ near $r = a$. In $\vec{S}_I = \vec{S}^{-} + \vec{S}^{-+} + \vec{S}^{+-}$ this weak flow gets cancelled at $z = \pm l$ by one of the cross-power flows. These last mutually cancel each other inside the unit cell, contributing significantly to the P-flow each.

In the waveguide $d = 0.9$, $a = 2$, H_{02} $(d\kappa/d\kappa\alpha < 0)$, $\kappa\alpha = 0.4$, Fig. 11, there is a curl around $\{r \approx a/2,\ z = 0\}$ in the back-flowing power $\vec{S}_R = \vec{S}^{+}$. The waveguide $d = 1.2$, $a = 1.4$, H_{03}, $(d\kappa/d\kappa\alpha < 0)$, $\kappa\alpha = 0.34$ is shown in Fig. 12. Here, the mode H_{03} is inverted, with a curl around $\{r = a,\ z = 0\}$ in $\vec{S}$.

Upon the lowest plotting in Fig. 13, there are the power flows $P_T(\kappa\alpha)$, $P_I(\kappa\alpha)$, H_{02}, $l = 3$, $a = 2$ at $d = 0.9$ -solid, $d = 2.425$ -dotted, $d = 1.44$ -dashed lines. In $d \in \{0.9, 2.425\}$ there are the maximums and in $d = 1.44$ the minimum of $\Delta\omega_2(\theta)$ from Fig. 5(b). The upper plots contain $P_T^M(\theta)$, $P_I^M(\theta)$ dependencies for H_{02} at $a = 2.8$ -solid, $a = 2.4$ -dashed, $a = 2$ -dotted lines.

This stop band $\Delta\omega_2$ is situated at $\kappa\alpha = 0$. The P_R flows are very strong in all of its maximums. In the minimum they equal zero, $P_R = 0$, $P_T = P_I$; and in this way, certain transparence conditions occur in the waveguide. These conditions are 'lengthy' by $\kappa\alpha$ (see the dashed lines upon the lower plotting).

As regards the Bragg bandwidth extremums, Fig. 13 demonstrates the equivalence in effect between the Brillouin diagram and the energy characteristic data.

In this way, all of the obtained numerical data are correct. In view of the information in Figs. 9–12, another implication can be that the employed space harmonic sub-setting at least does make physical sense, e.g., as a helpful model. But whether these sub-sets are physically independent or not, is yet unclear at this stage.

7. THE SHORT PERIODS IN PICW

Here, the contra-directional and the curl-like flows are most revealing. In particular, the contra-directional power flows, well-known concerning the PICW hybrid waves [12], have not been found regarding the symmetric types. Such flows, in our case those of H_{oi}-waves, do prove the very existence of the partials.

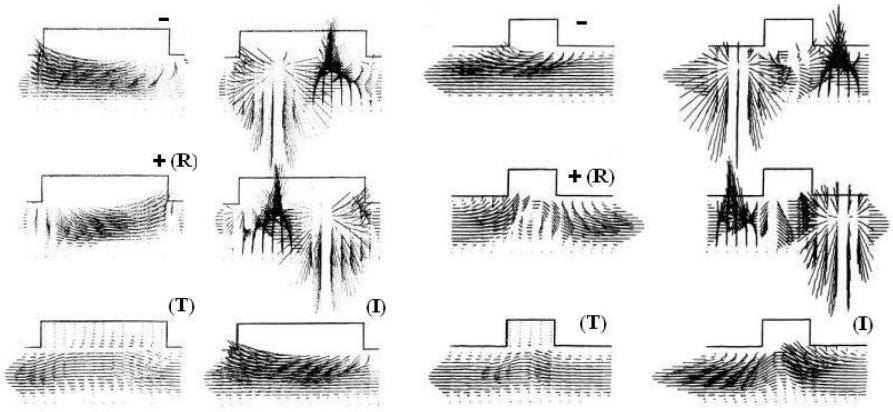

Figure 10. $\vec{S}$-vector ingredient flows (6) of the wave $d = 2.425$, $a = 2$, H_{o2}, $\kappa\alpha = 0.4$.

Figure 11. $\vec{S}$-vector ingredient flows (6) of the wave $d = 0.9$, $a = 2$, H_{o2}, $\kappa\alpha = 0.04$.

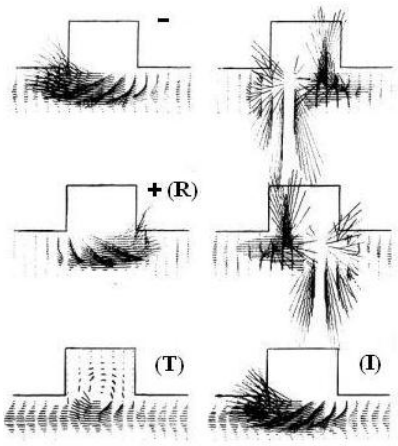

Figure 12. $\vec{S}$-vector ingredient flows (6) of the wave $d = 1.2$, $a = 1.4$, H_{o3}, $\kappa\alpha = 0.34$.

In Figs. 14–19 there are several typical examples of the vector $\vec{S}$-fields in PICW; $l = 0.75$, $d = 0.65$, $a \in \{2.6, 2.4, 2, 0.9\}$. All of these waves are the propagating ones; the contra-direction, curl-like, and the curl power flows are available.

The contra-direction flows in the flow $\vec{S}$ are triple-layered in Fig. 14 ($a = 2.6$, H_{03}, $\kappa\alpha = 0.18$), Fig. 16 ($a = 2.4$, H_{02}, $\kappa\alpha = 0.26$), Fig. 17 ($a = 2$, H_{04}, $\kappa\alpha = 0.32$), and double-layered in Fig. 15 ($a = 2.4$, H_{03},

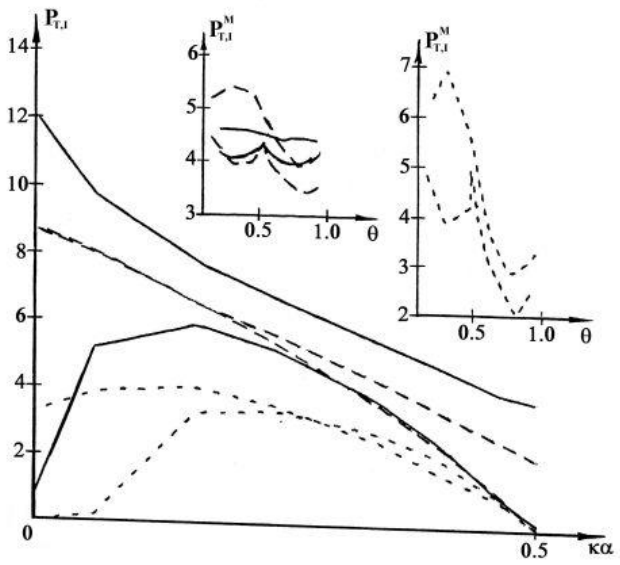

Figure 13. H_{o2}-mode, $l = 3$, $d = 2.8$: power flows P_T, P_I vs $\kappa\alpha$ at $\Delta\omega_2$ extremums, $a = 2$; and P_T^M, P_I^M vs θ, $a = 2.8, 2.4, 2$ (solid, dashed, dotted lines).

$\kappa\alpha = 0.18$).

The alternating contra-direction layers interchange energy between themselves. The power flows of the exchange are like curls within the propagation region in Figs. 14–16; though, only the flow in Fig. 16 has a closed flow-line. The power flow turbulence in Fig. 17 round ($r = a$, $z = 0$), or close to it, is even more curl-like. And there are definitely the curls in Fig. 18, $a = 0.9$, H_{03}, $\kappa\alpha = 0.3$, the curl is around ($r = a,\ z = 0$) or so, and in Fig. 19, $a = 0.9$, H_{04}, $\kappa\alpha = 0.26$, the curl rotates clock-wise around ($r > a$, $z = 0$). Both the H_{03} and H_{04} power flow r-spreads are like that of H_{01}-mode.

Further analysis, e.g., that of Fig. 17, demonstrates that the power $\vec{S}_R = \vec{S}^-$ flows backward ($z < 0$) and $\vec{S}^+$ flows forward ($z > 0$), and both flows are non-turbulent. The turbulence in $\vec{S}$ occurs due to the summing of $\vec{S}^{-+}$ and $\vec{S}^{+-}$, and is seen in the $\vec{S}_I$ power.

There is a curl around ($r = a,\ z = 0$) in $\vec{S}_I$ and an exchange turbulence of power between the two co-directed flow layers. Here, the contra-directed power flow originates only at the final summing $\vec{S} = \vec{S}_I + \vec{S}_R$.

The full analogy, in this respect, holds true for all the rest figures.

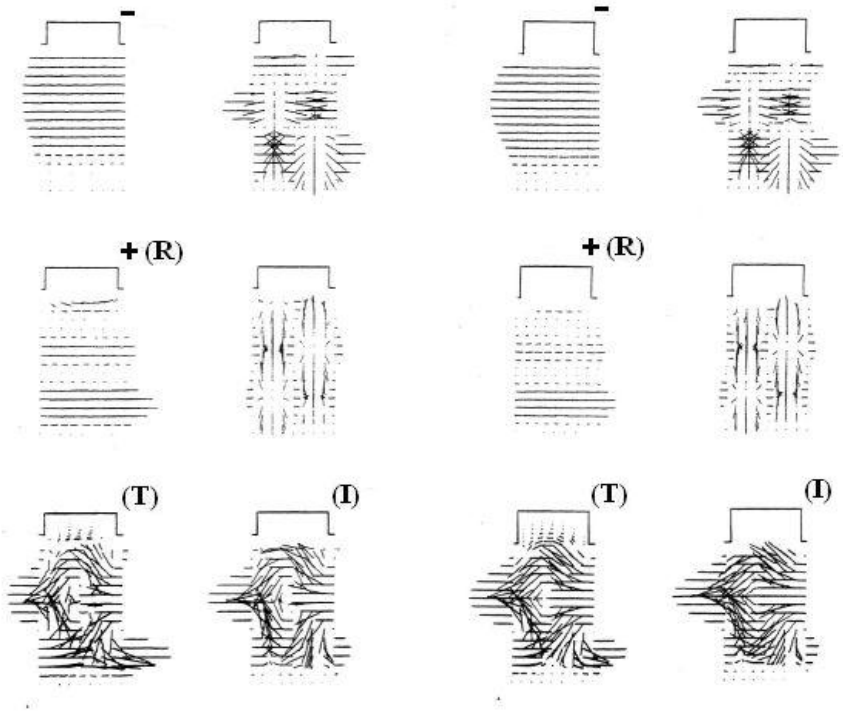

Figure 14. $\vec{S}$-vector ingredient flows (6) of the wave $a = 2.6$, H_{o3}, $\kappa\alpha = 0.18$. The contra-direction flows: 3 layers with the energy exchange.

Figure 15. $\vec{S}$-vector ingredient flows (6) of the wave $a = 2.4$, H_{o3}, $\kappa\alpha = 0.18$. The contra-direction flows: 2 layers with the energy exchange.

And this constructive contribution of each of the partials into the wave formation, actually proves their existence.

This is evidenced as well another way. The configurations of the power flows in $\vec{S}^-$ and $\vec{S}^+$ (EM fields) in Fig. 17, and all the other figures also, are in exact agreement with their 'original' mode form. This is about the process of the eigenmode H_{0i}, $i \geq 2$ forming after the *i.p.d.* in close vicinity to some 'inner' Bragg wave-point $0 < \kappa\alpha < 0.5$. Here, powers $\vec{S}^-$ and $\vec{S}^+$ are different in their r-symmetry. (Similar in between in their r-symmetry, the powers $\vec{S}^-$ and $\vec{S}^+$ obey, evidently, the same rules at $\kappa\alpha = 0, 0.5$).

When the periods are short, there are quite a number of the far-apart inner Bragg wave-points, and all of the physical mechanisms

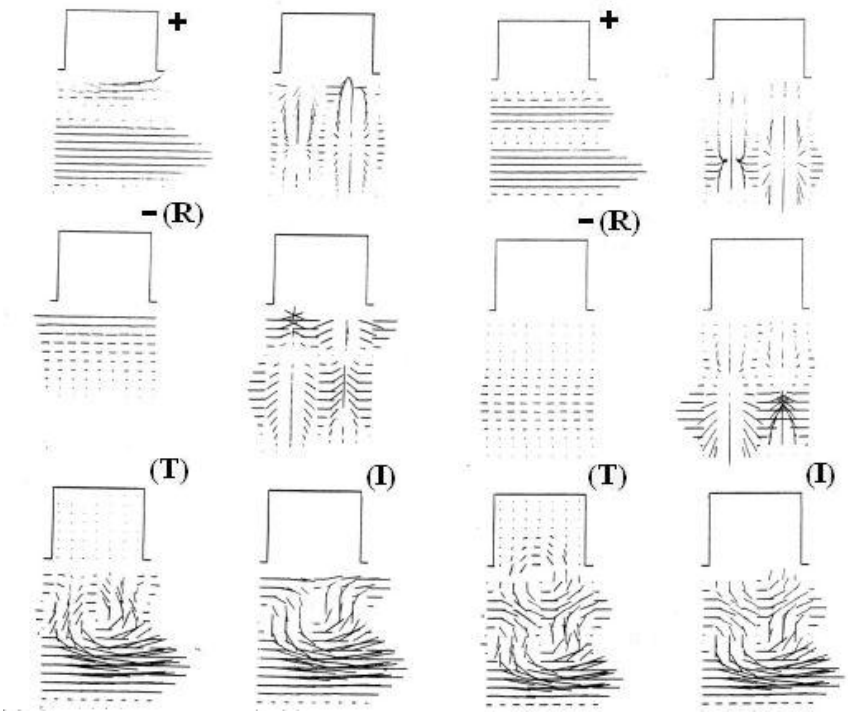

Figure 16. $\vec{S}$-vector ingredient flows (6) of the wave $a = 2$, H_{o2}, $\kappa\alpha = 0.26$. The contra-direction flows: 3 layers with the energy exchange.

Figure 17. $\vec{S}$-vector ingredient flows (6) of the wave $a = 2$, H_{o2}, $\kappa\alpha = 0.32$. The contra-direction flows; a curl-like turbulence close to $r = a$ in the wave power flow.

involved are fairly distinct; and, as a consequence, the partial waves are discerned for certain now.

The arbitrariness (e.g., regardless of the wavelength) of the Bragg wave-point possible position over $\kappa\alpha \in (0, 0.5)$ interval and the partial waves availability, reciprocally reconfirm each other. That is, wherever the regular modes cross each other, after the *i.p.d.*, then each Bragg wave-point gets formed after the pattern (6); representing, in this way, the relationship of equivalence.

It can thus be concluded:

The negative, $n < 0$, and the non-negative, $n \geq 0$, space harmonic sub-sets are the partial waves $\vec{S}^{-}$ and $\vec{S}^{+}$ of PICW eigenwave satisfying the relationship

$$\vec{S} = \vec{S}^{-} + \vec{S}^{+} + \vec{S}^{-+} + \vec{S}^{+-}. \tag{9}$$

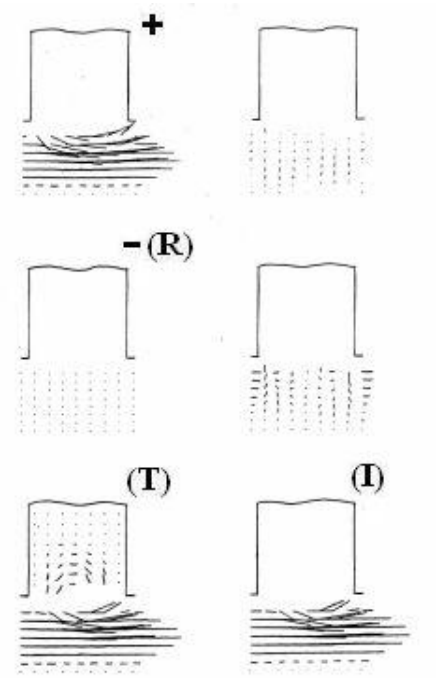

Figure 18. $\vec{S}$-vector ingredient flows (6) of the wave $a = 0.9$, H_{o3}, $\kappa\alpha = 0.3$. A curl is available in the wave power flow; and the reflected flow is slight. The Region-1 flow r-spread is like that of H_{o1}-wave.

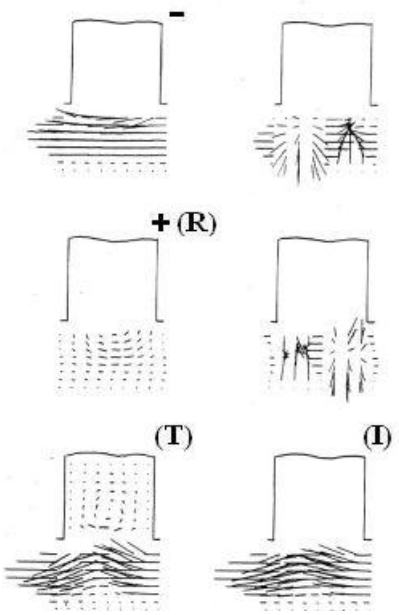

Figure 19. $\vec{S}$-vector ingredient flows (6) of the wave $a = 0.9$, H_{o4}, $\kappa\alpha = 0.26$. A curl is available inside the cell in the wave power flow, and there are the contra-directed to each other curls in $\vec{S}_R = \vec{S}^-$ and $\vec{S}^-$ near $r = a$. The Region-1 flow r-spread is like that of H_{o1}-wave.

In rigorous sense, this means, regarding the mathematical space-harmonic idealism, that physically the PICW eigenwave is such that the sub-sums $n < 0$ and $n \geq 0$, and only those sums, do make physical sense, constituting (i.e., in the monochrome event) the eigenwave partials. In other words, it is the physical interpretation of the PICW eigenwave.

The partials are constructively helpful in the eigenwave analysis. In particular, as regards the origination and physical interpretation of the PICW asymmetric wave hybridity. According to (5), (9), the regular asymmetric wave dispersion tree, Fig. 2, under the *i.p.d.*, does

appropriately form each of the PICW asymmetric eigenmodes (i.e., for each of the inner Bragg wave-points) due to a superimposing of one entirely H-mode and one entirely E-mode partials.

8. CONCLUSION

The occupational role of PICW in the PBS class is quite substantial; and so is the waveguide's one on its own. Evidently, only a special study can result in the adequate PICW electromagnetic theory, which is in fact missing for the moment; the numerical solutions to both the dispersion and the wave equations being fairly instrumental all together.

The dispersion and the energy aspects of the PICW eigenwave propagation are considered in a general way. The statement on the initial periodicity dispersion (5) and that concerning the partial wave concept (9) are the results. Some relevant categorization and notification are provided also; for example, concerning the regular and the periodicity modes, Bragg wave-point, Bragg wave-band, and etc.

Also, the classification of PICW eigen- values and modes, including the eigenwave total number formula, is obtained; as well as some exact information on the domineering role of the period-value, on the Bragg band extremums, the contra-directional, curl-like and other sorts of power flows on the symmetric waves, and etc. Certain physical interpretations are provided, such as that on the arbitrariness of the Bragg wave-point possible position over $\kappa\alpha[0, 0.5]$ interval, i.e., regardless of the wavelength; and also, as regards the mechanism of the PICW asymmetric waves hybridity.

A range of various power flow configurations and particularities as for the $\vec{S}^{-}$, $\vec{S}^{+}$ components, do represent a multitude of the eigenwave processes in the structure.

All of the results presented are valid to the whole PBS class.

It is some future task to go about the individual wave-type features, in order to substantiate properly all of the facts pointed out in the introduction.

ACKNOWLEDGMENT

The author is thankful to Prof. O. A. Tretyakov for useful discussions and encouragement; and to the colleagues, and many other friendly people for their help at his work in V. N. Karazin Kharkov National University.

REFERENCES

1. Chu, E. L. and W. W. Hansen, "The theory of disk-loaded wave guides," *Journal of Applied Physics,* Vol. 18, 996–1008, 1947.
2. Vladimirsky, V. V., "The propagation of radiowaves along the chain of endovibrators," *Zhurnal Tekhnicheskoy Phyzyki,* Vol. 17, 1269–1277, 1947 (in Russian).
3. Walkinshaw, W., "Wave guides for slow waves," *Journal of Applied Physics,* Vol. 20, 634–635, 1948.
4. Akhiezer, A. I. and J. B. Feinberg, "Slow electromagnetic waves," *Uspekhy Physicheskikh Nauk,* Vol. 44, 321–364, 1951 (in Russian).
5. Neal, R. B., "Design of linear electron accelerators with beam loading," *Journal of Applied Physics,* Vol. 29, 1019–1024, 1958.
6. Combe, R. and M. Feix, "Resultats theoretiques et experimentaux councernant les guides d'ondes charges et les pertiellment coaxiales," *Nuovo Cimento,* Vol. 15, 760–773, 1960.
7. Valdner, O. A. and A. V. Shalnov, *Electromagnetic Fields in the Iris-Loaded Waveguides of the Electron Linear Accelerators,* Gosenergoizdat, Moscow, 1963 (in Russian).
8. Saxon, G., T. R. Jarvis, and I. White, "Angular dependent mode in circular corrugated waveguide," *Proc. IEEE,* Vol. 51, 1365–1373, 1963.
9. Nishikava, T., S. Giordano, and D. Carter, "Dispersion relation and frequency characteristics of alternating periodic structure for linear accelerators," *Rev. Sci. Instrum.,* Vol. 37, 652–660, 1966.
10. Burshtein, E. A. and G. B. Voskresensky, *The Intensive Beam Electron Linear Accelerators,* Atomizdat, Moscow, 1970 (in Russian).
11. Hahn, H., Ch. I. Goldshtein, and W. Bauer, "On the theory of iris-loaded waveguides," *AEV,* Vol. 30, Nos. 7–8, 297–302, 1976.
12. Valdner, O. A., N. P. Sobenin, B. V. Zverev, and I. S. Schedrin, *The Guide to the Iris-loaded Waveguides*, O. A. Valdner (ed.), Atomizdat, Moscow, 1977 (in Russian).
13. Bruice, L., "Ten-times increase of TWT power," *Electronika,* Vol. 54, 12–13, 1981 (in Russian).
14. Kovalev, N. F., M. I. Petelin, M. D. Reizer, and A. V. Smorgonsky, "'O'-type devices based on the induced Cherenkov's and the transitional radiation of the relativistic electrons," *Relativistic Micro-wave Electronics,* 76–113, Publ. of the Institute of Applied Physics of Acad. of Sci. of the USSR., Gorkiy, 1979 (in Russian).
15. Galuzo, S. U., "Dispersion properties investigation in the

electrodynamic system of the relativistic Cherenkov's generator," *Radiotekhnika i Electronika,* Vol. 27, 559–63, 1982 (in Russian).

16. Vanke, V. A., S. K. Lesota, V. M. Lopukhin, et al., "The non-linear analysis in the TWT with transverse interaction and synchronized wave," *Radiotekhnika i Electronika,* Vol. 21, 149–158, 1976 (in Russian).
17. Clarricoats, P. I. B. and G. T. Poulton, "High-efficiency microwave reflector antennas," *A. Review. Proc. IEEE,* Vol. 65, 1470–1504, 1977.
18. Clarricoats, P. I. B., "Feeds for reflector antennas. A. Review," *Proceedings of Second Intern. Conference on Antennas and Propag., Part I: Antennas,* 309–317, University of York, York, London, UK, 1981.
19. Clarricoats, P. I. B., A. D. Olver, C. G. Parini, and G. T. Poulton, "Corrugated waveguide feeders for microwave antennas," *Advanced Antenna Technology,* 240–244, P. I. B. Clarricoats (ed.), MEPL, London, 1981.
20. Elachi, C., "Waves in active and passive periodic structures," *Proc. IEEE,* Vol. 64, 1666–1698, 1976.
21. Toyama, H. and K. Yasumoto, "Electromagnetic scattering from periodic arrays of composite circular cylindrer with internal cylindrical scatterers," *Progress In Electromagnetics Research*, PIER 52, 321–333, 2005.
22. Aissaoui, M., J. Zaghdoudi, M. Kanzari, and B. Rezig, "Optical properties of the quasi-periodic one-dimensional genarilized multilayer Fibonacci structures," *Progress In Electromagnetics Research*, PIER 59, 69–83, 2006.
23. Khalaj-Amirhosseini, M., "Scattering of inhomogeneous two-dimensional periodic dielectric gratings," *Progress In Electromagnetics Research*, PIER 60, 165–177, 2006.
24. Watanabe, K. and K. Kuto, "Numerical analysis of optical waveguides based on periodic Fourier transform," *Progress In Electromagnetics Research*, PIER 64, 1–21, 2006.
25. Melezhik, P. N., A. Y. Poyedinchuk, N. P. Yashina, G. Granet, and M. Ney, "Radiation from surface with periodic boundary of metamaterials excited by a current," *Progress In Electromagnetics Research*, PIER 65, 1–14, 2006.
26. Garault, Y., "Étude d'une classe d'ondes électromagnetique guidées: les onde EH. Application aux dèflectuers haute frèquence de particules rapides," *Annales de Physiques,* Vol. 10, 641–672, 1965.

27. Katenev, S. K., "Electromagnetics of simplest H-eigenwaves in periodic iris-loaded circular waveguide," *U.R.S.I. International Symposium "Mathematical Methods in Electromagnetic Theory-94" Conference Proceedings,* 164–167, Kharkov, Ukraine.
28. Katenev, S. K., "Electromagnetics of H-eigenwaves in periodic iris-loaded circular waveguide," *Proceedings of the U.R.S.I. International Symposium on Electromagnetic,* 38–40, St. Petersburg, Russia.
29. Collin, R. E., *Field Theory of Guided Waves,* 2nd ed., 851, IEEE Press, 1990.
30. Whitham, J. B., *Linear and Nonlinear Waves,* A Wiley-Interscience Publication, John Wiley & Sons, 1974.
31. Katenev, S. K., "Waves in periodic layered waveguides," *International Journal of Infrared and Millimeter Waves,* Vol. 16, 1825–1835, 1995.
32. Tretyakov, O. A., "Waveguide evolutionary equations," *Radiotekhnika i Electronika,* Vol. 34, 917–926, 1989 (in Russian).
33. Tretyakov, O. A., "Essentials of nonstationary and nonlinear electromagnetic field theory," *Analytical and Numerical Methods in Electromagnetic Wave Theory,* 123–145, M. Idemen, M. Hashimoto, and O. A. Tretyakov (eds.), Science House, Tokio, 1993.
34. Pierce, G. R. and P. K. Tien, "Coupling of modes in helices," *Proc. IRE.,* Vol. 37, 1389–1396, 1954.
35. Pierce, G. R., "Coupling of modes of propagation," *Journal of Applied Physics,* Vol. 25, 179–183, 1954.
36. Yeh, P., A. Yariv, and C.-S. Hong, "Electromagnetic propagation in periodic stratified media," *Journal of Optical Society of America,* Vol. 67, 423–448, 1977.
37. Yariv, A. and A. Grover, "Equivalence of the coupled mode and Floquet-Bloch formulation in periodic optical waveguides," *Applied Physics Letters,* Vol. 26, 537–539, 1975.
38. Yariv, A. and P. Yeh, "Optical waves in crystals," A Wiley-Interscience Publication, John Wiley & Sons, 1984.